CHINESE OPTICS LETTERS

Vol. 22, No. 3 | March 2024

22 kW near-diffraction-limited Yb:YAG slab laser amplifier without adaptive optics correction

Dan Wang (汪 丹)[1,2,3*], Ping He (何 平)[2], Tangjian Zhou (周唐建)[2], Mi Li (李 密)[2], Yingchen Wu (邬映臣)[1,2,3], Yanan Wang (王亚楠)[2], Jianli Shang (尚建力)[2**], Qingsong Gao (高清松)[2], Kai Zhang (张 凯)[2], Chun Tang (唐 淳)[2], and Rihong Zhu (朱日宏)[1]

[1] School of Electronic and Optical Engineering, Nanjing University of Science and Technology, Nanjing 210094, China

[2] Institute of Applied Electronics, China Academy of Engineering Physics, Mianyang 430079, China

[3] Graduate School of China Academy of Engineering Physics, Beijing 100193, China

*Corresponding author: 20930103@zju.edu.cn

**Corresponding author: shangjianli@outlook.com

Received October 15, 2023 | Accepted October 31, 2023 | Posted Online March 21, 2024

A high-power CW Yb:YAG slab laser amplifier with no adaptive optics correction has been experimentally established. At room temperature, the amplifier emits a power of 22 kW with an average beam quality (β) of less than 3 in 0.5 min. To our knowledge, this is the brightest slab laser without closed-loop adaptive optics demonstrated to date. In addition, an extracted power of 17 kW with an optical extraction efficiency of 33%, corresponding to a residual optical path difference of less than 0.5 μm, is achieved with the single Yb:YAG slab gain module. The slab gain module has the potential to be scalable to higher powers while maintaining good beam quality. This makes a high-power solid-state laser system simpler and more robust.

Keywords: laser amplifier; Yb:YAG; slab laser; surface quality; pumping uniformity.

DOI: 10.3788/COL202422.031402

1. Introduction

Lasers with high average power and beam quality are promising sources for materials processing, scientific research, and military defense[1–4]. The conduction-cooled end-pumped slab (CCEPS) configurations have the potential to provide high average power and high beam quality because the zigzag propagation in CCEPS eliminates the thermo-optical path difference (OPD) over the entire beam area[5–9]. Northrop Grumman Corporation, using Nd:YAG CCEPS, first realized more than 100 kW output power in 2009[10,11]. However, the 100 kW laser system with more than 30 slab gain modules (SGMs) was complex and lacked robustness due to the limitation of power extraction from a single SGM.

Yb:YAG is a promising alternative to Nd:YAG for high-average power operation because of its smaller quantum defect and simple electronic structure, resulting in lower volumetric heat generation. In 2001, Goodno *et al.*[12] first demonstrated a 3-mm-width Yb:YAG CCEPS laser, emitting a power of 252 W with beam quality factors (M^2) below 1.5. In 2006, Lu *et al.* presented a corner-pumped Yb:YAG slab laser that produced a power of 530 W with M^2 of 4.3 in a zigzag direction[13]. However, the quasi-three-level nature of Yb:YAG at room temperature makes the lasing threshold high. Under intense pumping and input power, the aggressive thermal effects, such as thermal-induced wavefront distortion and surface damage, limit the output power and degrade the output beam quality. In 2016, Chen *et al.* reported a MOPA configuration based on a 10-mm-width Yb:YAG CCEPS, which achieved an extraction power of 2.8 kW, but the beam quality was not measurable due to the poor OPD[14]. To simultaneously achieve high average power and high beam quality output, the adaptive optics (AO) system was employed for wavefront correction to improve the beam quality. In 2018, Xu *et al.* first demonstrated a two-stage Yb:YAG CCEPS MOPA chain with the AO system, obtaining 11.9 kW output power with the beam quality (β) improved from 9.8 to 2.8. The 30-mm-width SGM in the main amplifier was extracted with a maximum power of 8.3 kW[15]. In the same year, Wang *et al.* reported a three-stage Yb:YAG CCEPS MOPA chain with an AO system, realizing 22.3 kW output with β enhanced from 9.2 to 3.3. The second 30-mm-width SGM in the main amplifier was extracted with a maximum power of 11.3 kW[16]. In 2020, Huang *et al.* used a four-stage Yb:YAG slab AO-controlled MOPA system, obtaining 21.2 kW laser with a horizontal beam quality (HBQ) improved from 4.2 to 1.9. The single SGM was extracted with a maximum

© 2024 Chinese Optics Letters

power of 5.3 kW[17]. Although the output performance of AO-controlled Yb:YAG slab laser amplifiers is excellent, the addition of a downstream AO system increases the complexity of laser systems.

In this paper, we experimentally establish a two-stage Yb:YAG CCEPS MOPA chain without an AO system at room temperature, simultaneously achieving an output power of 22 kW and an average beam quality (β) of 2.95 in 0.5 min. To our knowledge, this is the brightest slab laser without the closed-loop AO system demonstrated to date. By improving the surface quality of the slab and the pumping uniformity of the long-distance transmission within the slab, the SGM in the main amplifier is extracted to 17 kW output power with 33% optical extraction efficiency, as well as less than 0.5 μm OPD of single-pass through the slab. In addition, the power extracted from the SGM is further increased by enlarging the width of the slab. With the improved SGM, the high-power laser system could become simpler and more robust.

2. Experimental Setup

The experimental setup of a two-stage Yb:YAG slab MOPA chain is shown schematically in Fig. 1. A Yb-doped fiber laser, a Yb:YAG CCEPS preamplifier, and a main amplifier form the main parts of the MOPA chain, making it power-scalable.

The seed of the MOPA chain is the high-power fiber laser with an output power of 1 kW, a beam quality (M^2) of 1.3, a wavelength of 1030 nm, and a linewidth (FWHM) of 0.3 nm. To protect the fiber laser from feedback, the fiber laser was designed as a linear polarization output with an extinction ratio (ER) $>$ 20 dB. The beam from the fiber laser was expanded and coupled into the Faraday isolator, and then shaped to 1.8 mm × 19 mm by beam shaper 1 (BS1) to match the end profile of the slab in the preamplifier. Based on previous studies[18,19], after three angular and multiplexing passes through the slab in the preamplifier, we obtained a high-brightness preamplifier with an output power of 5 kW and a beam quality (β) of 1.8.

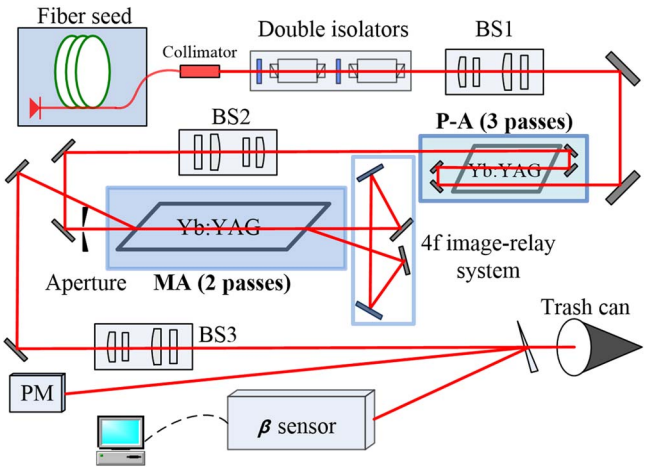

Fig. 1. Experimental setup of Yb:YAG slab MOPA chain. P-A, preamplifier; MA, main amplifier; BS, beam shaper; PM, power meter.

The output beam from the preamplifier is shaped by BS2 to 2.5 mm × 38 mm and imaged to match the end profile of the slab in the main amplifier. The high-power inputs to the preamplifier and main amplifier increase the energy storage extraction and reduce the residual gain to suppress the parasitic oscillations. After two angular and multiplexed passes through the slab in the main amplifier, the laser beam was expanded to 40 mm × 80 mm by BS3 to measure output power and beam quality. In each Yb:YAG slab, the laser propagates in a zigzag pattern. Inside the preamplifier and the main amplifier, the laser propagates through a 4f image relay system. This system consists of two reflective lenses with 1 m focal length (FL). At the exits of the preamplifier, a 1.8 mm × 19 mm aperture is positioned to cut the serious aberration part of laser wavefront near the edges of the slab and reduce the backward amplification in the preamplifier. The power loss of the aperture is less than 3%.

Both the SGMs in the preamplifier and main amplifier are the CCEPS configurations. The schematic of a single CCEPS is shown in Fig. 2(a). The pump source is a high-power laser diode array (LDA) with a central wavelength of 940 nm, a spectral width of 5 nm, and a maximum output power of 30 kW. The LDA at each end is delivered by the homogenized waveguide and coupling lens group, and then injected into the slab via TIR from the 45° end faces. The detailed scheme of pump coupling and homogenization system is denoted in Fig. 2(b). A fast axis focusing lens is employed to focus the pump light into the homogenized waveguide. The homogenized waveguide has dimensions of 200 mm(length) × 76 mm(width) × 7 mm(thickness) and is made of high purity fused silica (HPFS). The HPFS with OH-concentration of less than 1 ppm (parts per million) reduces the absorption for the 940 nm laser and the thermal effect. After passing through the homogenizing waveguide, the homogenized pump light is shaped and imaged in the slow-axis direction by two cylindrical

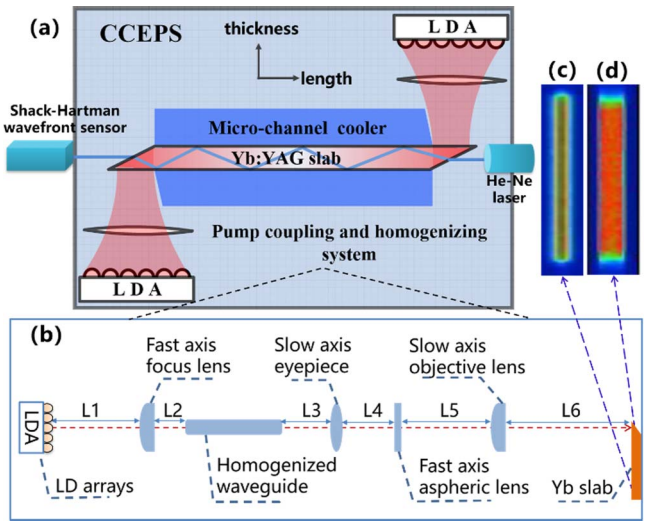

Fig. 2. (a) Schematic of CCEPS gain module; (b) detailed scheme of pump coupling and homogenization system; (c) and (d) distributions of pumping light at the middle of the slab and the entrance, respectively.

lenses, called a slow-axis eyepiece with FL = 100 mm and a slow-axis objective lens with FL = 50 mm, respectively. Both the cylindrical lenses have an anastigmatic design, which improves the uniformity of long-range transmission within the slab. In fast-axis direction, the homogenized pump light is focused by another cylindrical lens called a fast-axis aspheric lens with FL = 140 mm. The fast-axis aspheric lens with an aplanatic design enhances the energy concentration to reduce the waste heat at the end face of the slab. A simulation of the pumping light after passing through the homogenizing and coupling system is performed by Zemax. The distributions of the pumping light at the center and entrance of the slab are shown in Figs. 2(c) and 2(d), respectively, which illustrate that the homogeneities of the pumping light are well maintained along the length direction of the slab.

The slabs in the preamplifier and main amplifier are multi-concentration-doped, as shown in Fig. 3. The slab of preamplifier is 2 mm(thickness) × 20 mm(width) × 150 mm(length) in dimension, while that of the main amplifier is 2.5 mm(thickness) × 40 mm(width) × 150 mm(length) in dimension. The central 62-mm length of the slab is 0.42%-doped Yb:YAG, diffusion-bonded with two 34-mm long, 0.25%-doped Yb:YAG. To reduce the thermal effect and couple pump light into the slab, the rest of the slab is the diffusion-bonded undoped YAG, each of which is 10 mm long. The interfaces between the multi-concentration Yb:YAG slab, constructed by atomic diffusion bonding, have no visible scattered light under 532 nm laser irradiation. The wavefront distortion of slabs is less than 0.02λ/cm at 632.8 nm. The transmission loss is less than 0.3%/cm, which is the same as the intrinsic loss of YAG. The two end faces of the slab are at a 45° cut. The two edge faces of the slab are roughened and approximately parallel with an angle of 5° to suppress the amplified spontaneous emission (ASE) and parasitic oscillation. The two side faces of the slab are clipped and welded to the microchannel heat sinks for efficient cooling and dissipating heat, mainly produced by the quantum defect of Yb:YAG. Both the heat sinks are cooled by circulating water at the temperature of 20°C. However, each end face and side face with 5-mm-length undoped YAG are not cooled by the heat sinks because of the requirement of coupling the pump light.

For decreasing the thermal effect of the uncooled end caps of the slab in the main amplifier, the surface qualities of the slab are enhanced by the float-polishing (FP) method[20–23]. The defect sizes in the end face of the slab are reduced from 100 μm

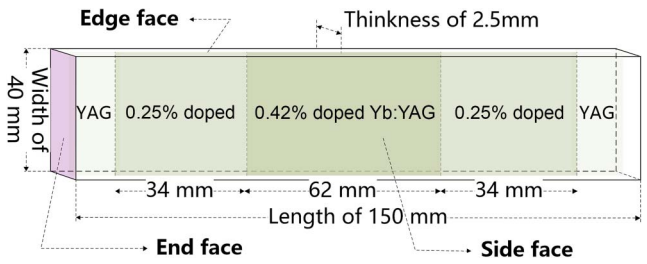

Fig. 3. Multi-concentration-doped slabs in the preamplifier and main amplifier.

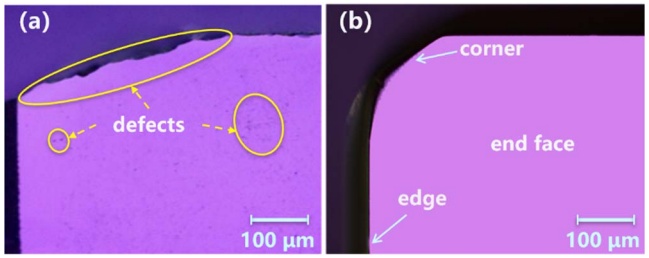

Fig. 4. Micrograph of the end face of the slab. (a) and (b) 100 μm level and submicrometer level surface, respectively.

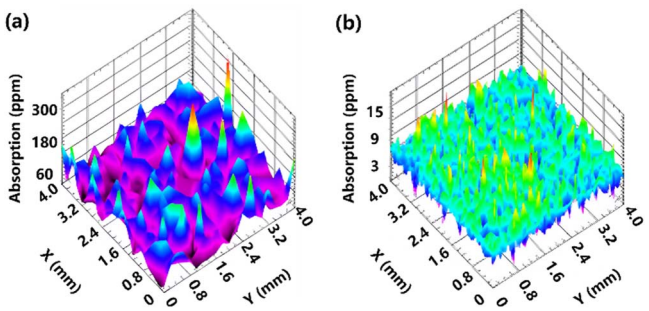

Fig. 5. Absorption rate of films. (a) and (b) Maximum absorption rate of 300 ppm and 20 ppm, respectively.

level to submicrometer level, as shown in Figs. 4(a) and 4(b). Meanwhile, the edge cracks in the stress-concentration regions of the slab, such as the corners and the edges, are dissipated by secondary chamfering and polishing, as shown in Fig. 4(b). Both the 45° end faces are antireflection (AR)-coated at 1030 nm and high-reflection (HR)-coated at 940 nm. The side face has a 3 μm SiO_2 film that is AR-coated at 940 nm and evanescent-wave-coated at 1030 nm. To reduce the thermal effects of the AR and HR films, the absorptivity and structural defects of the films are effectively reduced. The photothermal common-path interferometer (PCI)[24] is used to measure the absorption rate of the films. By optimizing the coating materials, evaporating ion source energy, and rate, the absorption rate of the films is reduced from 300 ppm to less than 20 ppm, as shown in Figs. 5(a) and 5(b).

3. Results and Discussion

Under the pump power of 15 kW without laser extraction, the end-face temperature of the main amplifier slab is reduced from 110°C to 40°C by improving the surface quality, as shown in Figs. 6(a) and 6(b). With the temperature reduction, the pump power could be increased, resulting in higher output power from a single slab.

At the input power of 5 kW, the output power of the MOPA chain and the optical extraction efficiency of the main amplifier are shown in Fig. 7(a). Under the pump power of 50 kW, the MOPA chain emits the maximum output power of 22 kW with

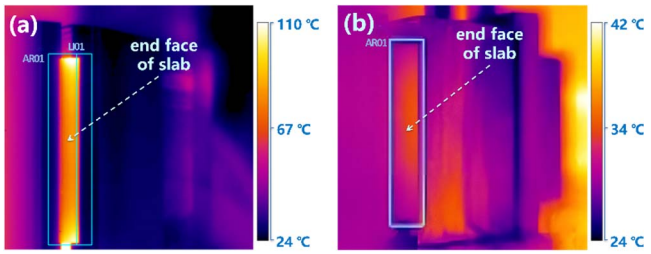

Fig. 6. Temperature comparison of the main amplifier slab end face. (a) and (b) Maximum temperatures of 110°C and 42°C, respectively.

an optical extraction efficiency of 34%. The optical extraction efficiency is defined here as the ratio of extracted amplifier power to total diode power. The experimental slope efficiency of 45% is achieved by linear fitting, as shown in Fig. 7(b). Based on previous simulation models of quasi-three-level Yb:YAG slab lasers[25–28], we calculate the theoretical output powers. The comparison of the theoretical and experimental dependence of the output power on the pump power is depicted in Fig. 7(b). The theoretical and experimental results show a good agreement, both of which illustrate the output powers could be further scaled linearly, as there are no obvious gain saturation effects.

Benefiting from the improvement of slab surface quality and pumping uniformity, the extraction power of SGM is up to 17 kW, which is much higher than that of other slab lasers. Owing to the CCEPS configuration with the ability of the power scalability by enlarging the width of slab, the power of 42.5 kW could be achieved by using a 10-cm-width slab. With the high-performance SGM, it is possible to reduce the number of slabs in a high-power laser system, making the laser simpler and more robust.

A Shack–Hartman wavefront sensor and a He–Ne laser are used to measure the OPDs of the slab, as shown in Fig. 2(a). The OPD of one passing through the slab at the maximum output power of 22 kW is displayed in Fig. 8(a). In the width direction of the slab, the peak-to-valley (PV) value of the OPD is 5.6 μm. By using quadratic fitting to eliminate defocus, the residual OPD is less than 0.5 μm, depicted in Fig. 8(b). Usually, the influence of defocus on the beam quality could be eliminated by the precompensation approach in experiment.

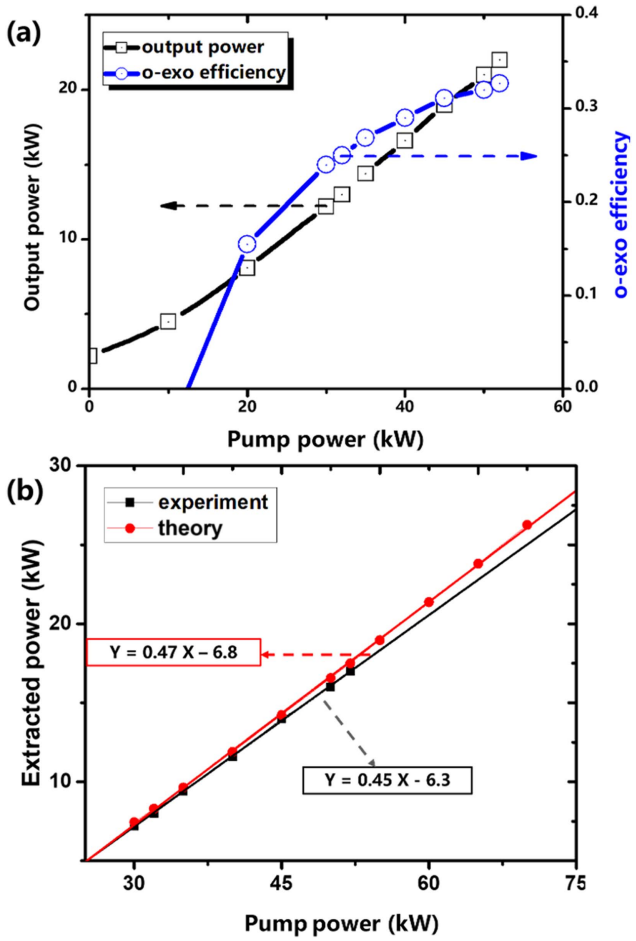

Fig. 7. (a) Output power of MOPA chain and optical extraction efficiency of main amplifier; (b) comparison of the theoretical and experimental dependence of the output power and slope efficiency.

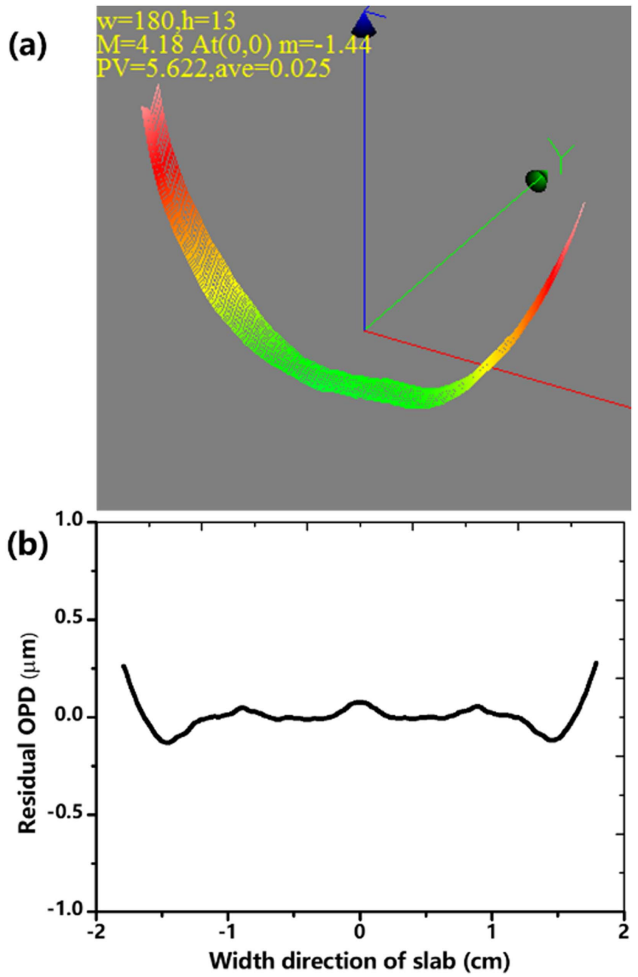

Fig. 8. (a) OPD of one passing through the slab at the maximum output power; (b) residual OPD after quadratic fitting to eliminate defocus.

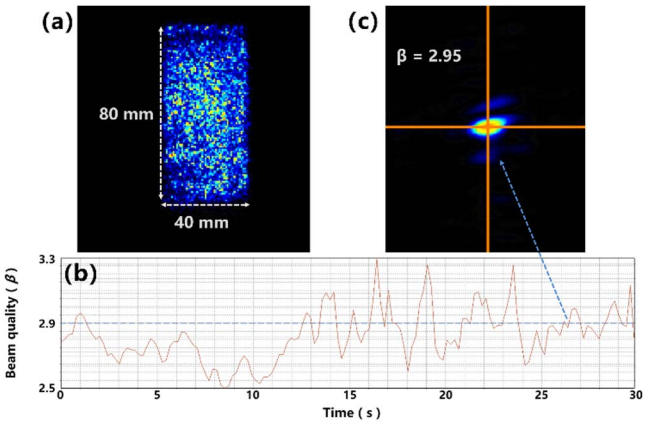

Fig. 9. (a) Distribution of the expanded beam in the near field; (b) variation of output beam quality (β) in 0.5 min; (c) far field with the beam quality of 2.95.

The residual OPD with the low spatial-frequency component in the middle region of the slab indicates little thermal-induced wavefront distortion, leading to a good beam quality of the output beam. Moreover, due to the zigzag propagation compensating the thermal effects, the OPD in the thickness direction is negligible.

For subsequent laser applications, the output beam of the MOPA chain is expanded to a rectangle of 40 mm × 80 mm by the BS3. The distribution of the expanded beam in the near field is shown in Fig. 9(a). The aberrations of defocus and tilt in the expanded beam are mostly eliminated by adjusting the distances and orientations between the two lenses in BS3. The beam quality of the expanded beam is measured by a β sensor. Under maximum output of 22 kW, the average value of β is 2.95 in 0.5 min, for which the minimum is 2.5 while the maximum is 3.3, as shown in Fig. 9(b). The beam profile with beam quality of 2.95 in the far field is exhibited in Fig. 9(c).

4. Conclusion

In this paper, by improving the surface quality of the slab and the uniformity of the pump beam to suppress the thermal effects, the load capacity and wavefront uniformity of the Yb:YAG slab are enhanced. With the SGM, the extraction power of single slab is up to 17 kW, and the residual OPD of a single pass is less than 0.5 μm. The MOPA chain without the AO system emitted an output power of 22 kW with an average β of 2.95 in 0.5 min. This is, to the best of our knowledge, the brightest slab laser without AO systems at room temperature demonstrated to date. Compared with the previous 20 kW level slab laser, the reduced number of SGMs and the absence of AO components reduce the complexity of the high-power MOPA chain and improve robustness.

Acknowledgements

This work was supported by the Joint Fund of the National Natural Science Foundation of China and the China Academy of Engineering Physics (No. U1830132), and the National Natural Science Foundation of China (No. 62105313).

References

1. T. Weyrauch, M. A. Vorontsov, G. W. Carhart, *et al.*, "Experimental demonstration of coherent beam combining over a 7 km propagation path," Opt. Lett. **36**, 4455 (2011).
2. Q. J. Gan, B. X. Jiang, P. D. Zhang, *et al.*, "Research progress of high average power solid-state lasers," Laser Optoelectron. Progress **54**, 010003 (2017).
3. P. Sprangle, B. Hafizi, and A. Ting, "NRL and the development of the laser weapon system," Future Force Nav. Sci. Technol. Mag. **2**, 18 (2015).
4. J. Deile, R. Brockmann, and D. Havrilla, "Current status and most recent developments of industrial high power disk lasers," in *Conference on Lasers and Electro-Optics/International Quantum Electronics Conference* (2009), paper CThA4.
5. X. Fu, Q. Liu, X. P. Yan, *et al.*, "End-pumped Nd:YAG zigzag slab laser with weak pump absorption," Chin. Opt. Lett. **7**, 492 (2009).
6. Q. Gao, H. L. Zhang, and J. Fayyaz, "Laser diode partially end-pumped electro-optically *Q*-switched Yb:YAG slab laser," Chin. Opt. Lett. **17**, 11 (2019).
7. J. Liu, Y. Liu, X. J. Tang, *et al.*, "A design of a surface-doped Yb:YAG slab laser with high power and high efficiency," Chin. Opt. Lett. **16**, 101401 (2018).
8. G. D. Goodno, H. Komine, S. J. McNaught, *et al.*, "Coherent combination of high-power, zigzag slab lasers," Opt. Lett. **31**, 1247 (2006).
9. M. Ganija, D. Ottaway, P. Veitch, *et al.*, "Cryogenic, high power, near diffraction limited, Yb:YAG slab laser," Opt. Express **21**, 6973 (2013).
10. J. Marmo, H. Injeyan, H. Komine, *et al.*, "Joint high power solid state laser program advancements at Northrop Grumman," in Proc. SPIE **7195**, 719507 (2009).
11. S. J. McNaught, C. P. Asman, H. Injeyan, *et al.*, "100-kW coherently combined Nd:YAG MOPA laser array," in *Frontiers in Optics 2009/Laser Science XXV/Fall 2009 OSA Optics & Photonics Technical Digest* (2009), paper FThD2.
12. G. D. Goodno, S. Palese, J. Harkenrider, *et al.*, "Yb:YAG power oscillator with high brightness and linear polarization," Opt. Lett. **26**, 1672 (2001).
13. F. Y. Lu, M. L. Gong, H. Z. Xue, *et al.*, "Optimizing the composite slab sizes in corner-pumped lasers," Opt. Laser Technol. **39**, 949 (2007).
14. X. M. Chen, L. Xu, H. Hu, *et al.*, "High-efficiency, high-average-power, CW Yb:YAG zigzag slab master oscillator power amplifier at room temperature," Opt. Express **24**, 24517 (2016).
15. L. Xu, Y. C. Wu, Y. L. Du, *et al.*, "High brightness laser based on Yb:YAG MOPA chain and adaptive optics system at room temperature," Opt. Express **26**, 14592 (2018).
16. D. Wang, Y. L. Du, Y. C. Wu, *et al.*, "20 kW class high-beam-quality CW laser amplifier chain based on a Yb:YAG slab at room temperature," Opt. Lett. **43**, 3838 (2018).
17. L. Huang, Y. M. Zheng, Y. D. Guo, *et al.*, "21.2 kW, 1.94 times diffraction-limit quasi-continuous-wave laser based on a multi-stage, power-scalable and adaptive optics controlled Yb:YAG master-oscillator-power-amplifier system," Chin. Opt. Lett. **18**, 061402 (2020).
18. Y. N. Wang, T. J. Zhou, J. L. Shang, *et al.*, "Yb slab laser amplifier with a laser output of 7.13 kW, 2 times diffraction limit," Laser Optoelectron. Progress **58**, 1114007 (2021).
19. M. Najafi, M. Shayganmanesh, M. M. Majidof, *et al.*, "Nd:YAG end-pumped zigzag multi-pass slab amplifier optimization: numerical and experimental study regarding the saturation effects," Opt. Express **30**, 16184 (2022).
20. Y. Namba and H. Tsuwa, "Ultrafine finishing of sapphire single crystal," Ann. CIRP **27**, 325 (1977).
21. J. M. Bennett, J. J. Shaffer, Y. Shibano, *et al.*, "Float polishing of optical materials," Appl. Opt. **26**, 696 (1987).
22. H. G. Gao, J. L. Cao, and B. Chen, "Float polishing for super smooth surface," Opt. Technique **21**, 40 (1995).

23. Z. L. Ma, L. R. Peng, and J. L. Wang, "Ultra-smooth polishing of high-precision optical surface," Optik **124**, 24 (2013).
24. K. V. Vlasova, A. I. Makarov, N. F. Andreev, *et al.*, "High-sensitive absorption measurement in transparent isotropic dielectrics with time-resolved photothermal common-path interferometry," Appl. Opt. **57**, 6318 (2018).
25. G. L. Bourdet, "Theoretical investigation of quasi-three-level longitudinally pumped continuous wave lasers," Appl. Opt. **39**, 966 (2000).
26. G. L. Bourdet, "Numerical simulation of the amplification of a short laser pulse by a ytterbium doped amplifier longitudinally pumped by short pump pulses," Appl. Opt. **45**, 4695 (2006).
27. D. Albach, J. C. Chanteloup, and G. Touzé, "Influence of ASE on the gain distribution in large size, high gain Yb^{3+}:YAG slabs," Opt. Express **17**, 3792 (2009).
28. L. Chen, Y. Liu, H. Zhao, *et al.*, "Multiphysics simulation of quasi-three-level end- pumped laser," Laser Infrared **50**, 58 (2020).